

Molecular approaches to photomagnetic materials. Metal-dependent regiospecificity in the exchange coupling of magnetic metal ions with the free radical substituents on pyridine base ligands*

Hiizu Iwamura^{1,†} and Noboru Koga²

¹*Institute for Fundamental Research of Organic Chemistry, Kyushu University, Hakozaki, Higashi-ku, Fukuoka 812-8581, Japan;* ²*Faculty of Pharmaceutical Sciences, Kyushu University, Maidashi, Higashi-ku, Fukuoka 812-8582, Japan*

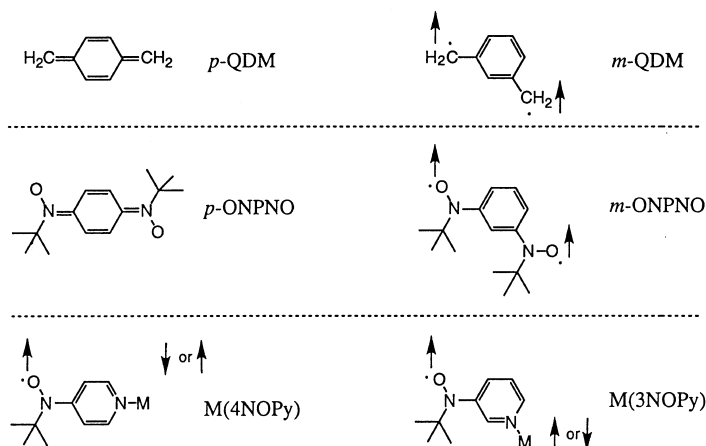
Abstract: Coordinatively unsaturated Cr(III), Mn(II) and Cu(II) complexes form with *N*-tert-butyl-*N*-(3- and 4-pyridyl)aminoxyls discrete complexes in which the pyridyl nitrogen atoms are coordinated to the metal ions. Magnetic susceptibility measurements revealed that the intramolecular exchange coupling between the magnetic metal ions and the aminoxyl group in the complexes is governed not only by the orientation of the π -spin-polarized pyridyl ring but also on the nature of the magnetic d-orbital of the metal ions. One-to-one chain polymer complexes were obtained from bis(hexafluoroacetylacetonato)manganese(II) and copper(II) with diazodi(4-pyridyl)methane. The weakly paramagnetic complexes were converted to ferri- and ferromagnetic chains, respectively, of considerable correlation length upon UV-irradiation.

INTRODUCTION

The classification of π -conjugated hydrocarbons into Kekulé and non-Kekulé hydrocarbons has proved to be most useful in understanding their electronic structures and properties. Whereas *o*- and *p*-quinodimethanes (QDM) and analogues, e.g. the Thiele hydrocarbon, are typical examples of the former and have closed-shell singlet ground states, *m*-quinodimethane and the Schlenk hydrocarbon belong to the latter and have triplet ground states resulting from the presence of two singly occupied nonbonding molecular orbitals [1]. The same is true for the corresponding heteroatom-centered diradicals; whereas the *p*-isomer has a quinone-diimine *N,N'*-dioxide structure (*p*-ONPNO) [2a], *m*-phenylenebis(*N*-tert-butylaminoxyl) (*m*-ONPNO) is a triplet species in the ground state [2b]. This orientational specificity in the exchange interaction between the two benzylic radical centers is derived from differences in the phase of the spin polarization of the π -electrons on the benzene ring and has served as an important guiding principle for designing super-high-spin polyradicals as prototypes for purely organic ferromagnets [3]. The construction of high dimensional molecular architecture showing reasonably high temperature for ferri- and/or ferromagnetic transitions has been achieved by a combination of bis(hexafluoroacetylacetonato)manganese(II) [Mn(hfac)₂] with *m*-ONPNO and analogous triradicals [4]. It is of great interest to know whether the 3d spin of the metal ions coordinated with *N*-(3- and 4-pyridyl)-*N*-tert-butylaminoxyls (3NOPy and 4NOPy) aligns in parallel or antiparallel with the 2p spin of the aminoxyl radical in the complexes [M(NOPy)] topologically similar to the isomeric QDM and ONPNO (Scheme 1).

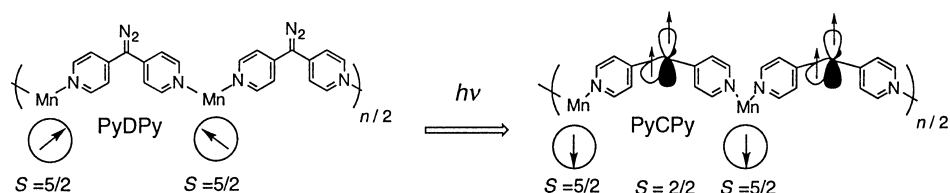
*Lecture presented at the 9th International Symposium on Novel Aromatic Compounds (ISNA-9), Hong Kong, China, 2–7 August 1998, pp. 209–302.

†Corresponding author: E-mail: iwamura@niad.titech.ac.jp



Scheme 1

The knowledge of the regioselectivity and the metal-dependence of the exchange coupling in the complexes thus obtained has been used to develop a strategy of incorporating the carbene centers into rigid polymeric metal complexes by combining $[M(\text{hfac})_2]$ ($M = \text{Mn}(\text{II})$ and $\text{Cu}(\text{II})$) with diazodi(4-pyridyl)methane (PyDPy) serving as a bridging ligand (Scheme 2). Their magnetic properties after photolysis will be discussed.



Scheme 2

RESULTS AND DISCUSSION

Discrete model complexes for studies of the metal-dependent regioselectivity in the exchange coupling between magnetic metal ions and radical centers attached on the pyridine bases

Preparation and X-ray crystal structures of the model complexes

When $[M(\text{hfac})_2]$ ($M = \text{Mn}(\text{II})$ and $\text{Cu}(\text{II})$) were allowed to react with ligands NOPy, *N*-[3- and 4-(1-imidazolyl)phenyl]-*N*-*tert*-butylaminoxyls (NOIm) and 4-(α -diazobenzyl)pyridine (4DPy) under mild conditions, 1:2 and 1:1 complexes were obtained [5]. Tetraarylporphyrinatochromium(III) chloride gave 1:1 complexes in which NOPy served as axial ligands [6].

A number of the complexes were obtained as single crystals amenable to X-ray crystal structure analyses. ORTEP drawings for two representative complexes are given in Fig. 1. The metal ions are typically in the center of elongated and/or distorted octahedra and the two pyridyl nitrogen atoms are attached to the metal ion in the *cis* or *trans* configuration. An examination of the bond lengths around the metal ions reveals that the $\text{N}(1)\text{-Mn-N}(1')$ bonds are on the elongation axes and correspond to the d_z orbital of $\text{Mn}(\text{II})$. The elongation axes lie along $\text{O}(1)\text{-Cu-O}(1')$ bonds in three copper complexes, indicating that the lobes of the magnetic $d_{x^2-y^2}$ orbital are directed toward the $\text{O}(1)$'s of the hfac units and $\text{N}(1)$'s of the pyridine units. The 1:1 complex $[\text{Mn}(\text{hfac})_2(4\text{NOPy})_2]$ was found to be a head-to-tail cyclic dimer.

Magnetic properties

The magnetic susceptibility data of the metal-radical complexes were obtained in the temperature range 2–300 K at a constant field of 100–800 mT on a Quantum Design MPMS2 SQUID susceptometer/

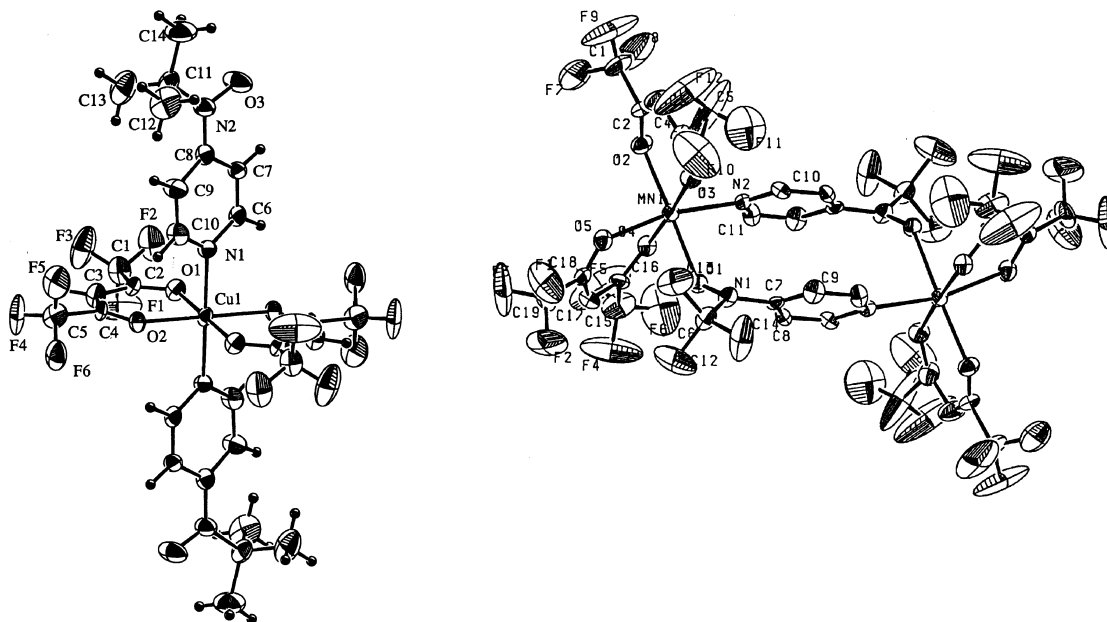


Fig. 1 ORTEP drawings of $[\text{Cu}(\text{hfac})_2(4\text{NOPy})_2]$ and $[\text{Mn}(\text{hfac})_2(4\text{NOPy})_2]$.

magnetometer. Typical results of the temperature dependence of the molar paramagnetic susceptibility χ_{mol} and their analyses are exemplified by $[\text{M}(\text{hfac})_2(4\text{NOPy} \text{ and } 3\text{NOPy})_2]$ in Fig. 2. A $\chi_{\text{mol}}T$ value of 1.29 emu/K/mol obtained at 300 K for $[\text{Cu}(\text{hfac})_2(4\text{NOPy})_2]$ is close to a theoretical 1.13 emu/K/mol calculated for three isolated $S=1/2$ spins $\{\chi_{\text{mol}}T = 0.125 \times g \times 2[3S(S+1)] = 0.125 \times 2 \times 2(3/2[1/2 + 1])\}$. As the temperature was decreased, $\chi_{\text{mol}}T$ values (open circles in Fig. 2a) increased gradually, reached a maximum at 36 K, and rapidly decreased below 10 K. A maximum $\chi_{\text{mol}}T$ value of 1.69 emu/K/mol is slightly smaller than a theoretical 1.87 emu/K/mol calculated for $S=3/2$. A linear three-spin model suggested by the X-ray crystal and molecular structure was adopted for analyzing the temperature dependence of the observed $\chi_{\text{mol}}T$ values more quantitatively. Its spin Hamiltonian is written as eqn 1:

$$H = -2J(S_1S_M + S_M S_2) \quad (1)$$

A Boltzmann distribution among the spin states given by the eigen values of eqn 1 for three spins with $S_1 = S_2 = S_M = 1/2$ was assumed and the theoretical equation thus derived was fitted to the experimental data by means of a least-squares method. The Weiss constant θ was used to represent by a mean-field theory a weak intermolecular interaction expected from the short contact of 5.85 Å in the crystal packing of the complex. The best-fit parameters were: $J/k_B = 60.4 \pm 3.3$ K, $g = 2.048 \pm 0.0091$, and

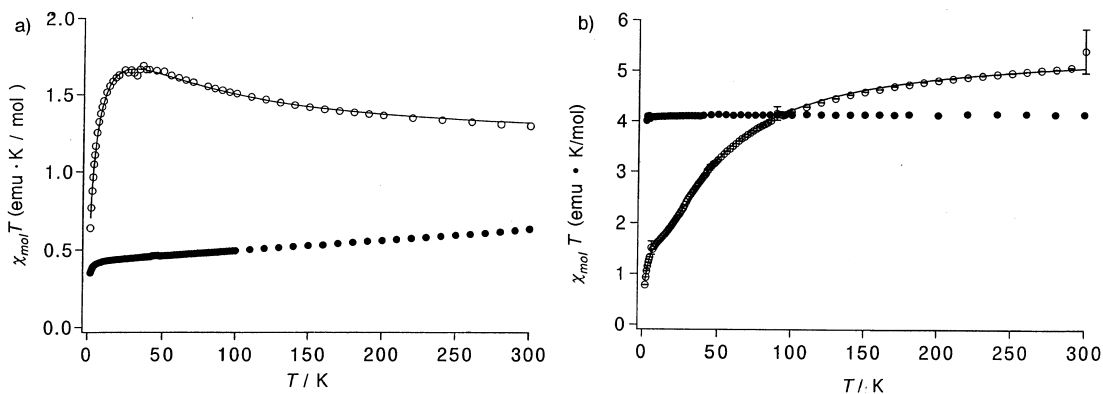


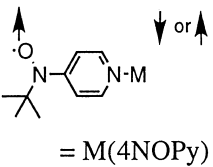
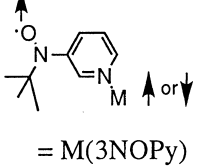
Fig. 2 Plots of $\chi_{\text{mol}}T$ vs. T for crystalline samples of: (a) $[\text{Cu}(\text{hfac})_2(4\text{NOPy})_2]$ (○) and $[\text{Cu}(\text{hfac})_2(3\text{NOPy})_2]$ (●) and (b) $[\text{Mn}(\text{hfac})_2(4\text{NOPy})_2]$ (○) and $[\text{Mn}(\text{hfac})_2(3\text{NOPy})_2]$ (●). Solid curves are the best-fit theoretical ones.

$\theta = -3.58 \pm 0.09$ K, where all symbols have their usual meaning. The fitted theoretical curve is presented by a solid curve in Fig. 2a.

A $\chi_{\text{mol}}T$ value for $[\text{Cu}(\text{hfac})_2(3\text{NOPy})_2]$ was ≈ 0.6 emu/K/mol at 300 K and gradually decreased to 0.43 at 10 K with decreasing temperature (filled circles in Fig. 2a). The observed values are close to a theoretical 0.37 emu/K/mol for $S = 1/2$. Cancellation of the two spins of the aminoxy radicals by a strong antiferromagnetic interaction between the neighboring complexes is suggested by the X-ray crystal structure of $[\text{Cu}(\text{hfac})_2(3\text{NOPy})_2]$. It appears in the $\chi_{\text{mol}}T$ vs. T plots as if the copper complex has no aminoxy radical units.

In the case of pairs of 1:1 complexes of (tetraarylporphyrinato)chromium(III) chloride with NOPy, a complementarity between the 3NOPy and 4NOPy is obvious (Table 1). The results of the other magnetic measurements and analyses are summarized in Tables 1 and 2.

Table 1 The exchange coupling parameters J/k_B (in K) in $M(\text{NOPy})$

M	 = M(4NOPy)	 = M(3NOPy)
Mn(II) $S = 5/2$	-12.4 K in $[\text{Mn}(4\text{NOPy})_2(\text{hfac})_2]$ -10.2 K in $[\text{Mn}(4\text{NOPy})_2(\text{acac})_2]$ -11.3 K in $[\text{Mn}(4\text{NOPy})(\text{hfac})_2]_2$? in $[\text{Mn}(3\text{NOPy})_2(\text{hfac})_2]$
Cu(II) $S = 1/2$	60.4 K in $[\text{Cu}(4\text{NOPy})_2(\text{hfac})_2]$ 58.6 K in $[\text{Cu}(4\text{NOPy})(\text{hfac})_2]_2$ 4.3 K in $[\text{Cu}(4\text{NOIm})_2(\text{hfac})_2]$	<-160 K in $[\text{Cu}(3\text{NOPy})_2(\text{hfac})_2]$ -2.7 K in $[\text{Cu}(3\text{NOIm})_2(\text{hfac})_2]$
Cr(III) $S = 3/2$	-77 K in $[\text{Cr}(\text{TPP})(4\text{NOPy})\text{Cl}]$ -86 K in $[\text{Cr}(\text{TAP})(4\text{NOPy})\text{Cl}]$	12.3 K in $[\text{Cr}(\text{TPP})(3\text{NOPy})\text{Cl}]$ 16.0 K in $[\text{Cr}(\text{TAP})(3\text{NOPy})\text{Cl}]$

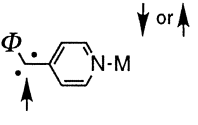
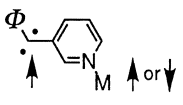
Plus and minus signs correspond to \uparrow and \downarrow spins at M, respectively.

Metal-dependent regioselectivity in the exchange coupling between the metal ions and the radical centers through the pyridyl ring

The metal-dependence

The observed exchange interaction of the magnetic metal ions with *N*-tert-butylaminoxy radicals (Table 1) and the triplet arylcarbenes (Table 2) through the 4-pyridyl ring clearly demonstrates that its

Table 2 The exchange coupling parameters J/k_B (in K) in $M(4\text{CPy})$ and $M(\text{PyCPy})$

M	 ↓ or ↑	 ↑ or ↓
Mn(II) $S = 5/2$	-17.8 K in $[\text{Mn}(4\text{CPy})_2(\text{hfac})_2]$ -17.4 K in <i>cis</i> - $[\text{Mn}(\text{PyCPy})_2(\text{hfac})_2]_n$ -12.3 K in <i>trans</i> - $[\text{Mn}(\text{PyCPy})_2(\text{hfac})_2]_n$	—
Cu(II) $S = 1/2$	33.4 K in <i>trans</i> - $[\text{Cu}(\text{PyCPy})_2(\text{hfac})_2]_n$	—

Plus and minus signs correspond to \uparrow and \downarrow spins at M, respectively.

The values for the polymers were obtained by a method extrapolating the corresponding small rings [7].

sign is determined by the kind of the metal ions: positive for copper(II) and negative for manganese(II) and chromium(III). A nature of the magnetic orbitals of the metal ions appears to play an important role in governing the sign of the coupling. We note that, whereas there are π -type magnetic orbitals in Cr(III) and Mn(II) that can overlap with the $2p\pi$ orbital at the pyridyl nitrogen atom in which the spin is polarized due to the presence of the aminoxyl radical, the magnetic orbital is $d_{x^2-y^2}$ and orthogonal to the $2p\pi$ orbital at the pyridyl nitrogen in the Cu(II) complexes. As in *p*-QDM and *p*-ONPNO in Scheme 1, the unpaired electrons should couple antiferromagnetically when the two orbitals concerned overlap at the pyridyl nitrogen. Hund's rule would predict the coupling to be ferromagnetic when they are orthogonal in the Cu(II) complexes (Fig. 3) [8].

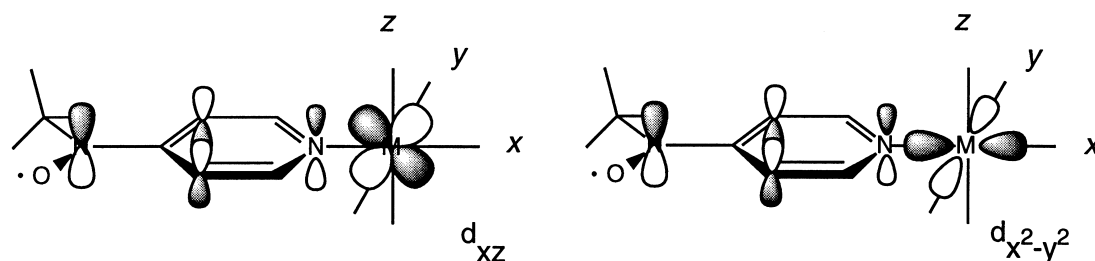


Fig. 3 Antiferro- and ferromagnetic coupling for the π - and σ -type magnetic orbitals, respectively, at M in 4NOPy-M.

Oriental specificity

Limited data on the sign of the coupling through the 3-pyridyl ring (Table 1) are in line with the idea that they can be opposite to those in 4NOPy. The sign of the polarization of the π -electrons due to the aminoxyl radical alternates on the pyridine ring and is therefore out of phase by one atom as in isomeric QDM and ONPNO in Scheme 1.

Photochemical generation of metal-radical complexes exhibiting ferri- and ferro-magnetic infinite chain characteristics. Molecular approaches to photomagnetic materials

Preparation and X-ray structures of the copper(II) and manganese(II) complexes

Solutions of diazodi(4-pyridyl)methane (PyDPy) in CH_2Cl_2 and $[\text{Mn}(\text{hfac})_2]$ in *n*-heptane or $[\text{Mn}(\text{hfac})_2 \cdot 2\text{H}_2\text{O}]$ in CH_2Cl_2 -methanol gave isomeric 1:1 complexes **a** and **b** of $[\text{Mn}(\text{hfac})_2 \cdot \text{PyDPy}]_n$ as red cubes and orange plates, respectively. $[\text{Cu}(\text{hfac})_2]$ in *n*-heptane-MeOH were mixed with PyDPy in a 1:1 molar ratio at room temperature. The resulting yellow-green precipitates were recrystallized from MeOH and MeOH- CH_2Cl_2 -benzene to give crystals **a** and **b** of $[\text{Cu}(\text{hfac})_2 \cdot \text{PyDPy}]_n$ as yellow-green plate and dark green brick,

Samples **a** and **b** of $[\text{Mn}(\text{hfac})_2 \cdot \text{PyDPy}]_n$ were too fragile to stand ambient temperature measurements and therefore their molecular and crystal structures have been solved by X-ray analysis using an imaging plate at -100 and -80 °C, respectively. The coordination geometry with respect to two pyridyl nitrogens is *cis* and *trans*, respectively (Fig. 4). Complex **a** of $[\text{Cu}(\text{hfac})_2 \cdot \text{PyDPy}]_n$ looked very similar to the latter. Single crystals of complex **b** were not obtained due to the limited quality of the crystals and the lability of the crystal due to included solvents of crystallization. Complexes **a** of $[\text{Mn}(\text{hfac})_2 \cdot \text{PyDPy}]_n$ has a helical one-dimensional chain.

Magnetic properties before and after irradiation

Temperature dependencies of χ_{mol} for $[\text{Mn}$ - and $\text{Cu}(\text{hfac})_2 \cdot \text{PyDPy}]_n$ in the range 2–300 K were measured at constant fields of 50 and 500 mT below and above 70 K, respectively. The results are shown in Fig. 5.

Before irradiation, $\chi_{\text{mol}}T$ values of a fine crystalline sample of complex **a** of $[\text{Mn}(\text{hfac})_2 \cdot \text{PyDPy}]_n$ were nearly constant at 2–300 K and its value is close to a theoretical spin-only value of 4.37 emu/K/mol expected for paramagnetic samples of $S=5/2$. After photolysis with the light ($\lambda=514$ nm) from an Argon ion laser through an optical fiber inserted into SQUID at about 5 K, $\chi_{\text{mol}}T$ values gradually

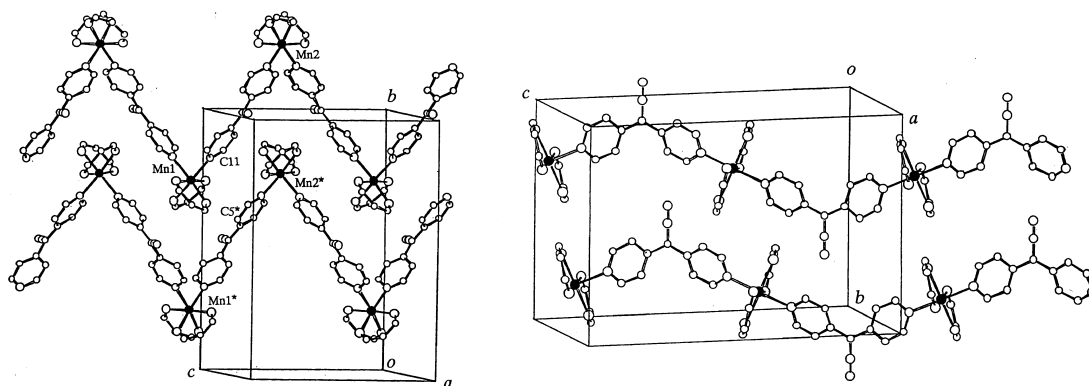


Fig. 4 Ball and stick drawings of the crystal structures for complexes **a** and **b** of $[\text{Mn}(\text{hfac})_2 \cdot \text{PyDPy}]_n$, respectively.

decreased with decreasing temperature to a shallow minimum of 3.58 emu/K/mol at ≈ 80 K, rapidly increased, reached a maximum of 32.2 emu/K/mol at 3 K, and then decreased. An irreversible change in the $\chi_{\text{mol}}T$ values was observed at 230 K above which they traced the horizontal line before irradiation. Subsequent measurement of the $\chi_{\text{mol}}T$ values at 2–300 K of the same sample showed temperature independent horizontal lines overlapped with those before irradiation. The magnetic behavior after irradiation is consistent with the formation of ferrimagnetic chains; the correlation of increasing length reached 186 and 218 $S=3/2$ units at 5 and 1.9 K for complexes **a** and **b**, respectively. The $\chi_{\text{mol}}T$ vs. T plots were analyzed theoretically on the basis of a ferrimagnetic chain model consisting of a $S=5/2$ classical and $S=2/2$ quantum spins to give J/k_B values summarized in Table 2 [7].

Before irradiation, $\chi_{\text{mol}}T$ values for crystalline samples **a** and **b** of $[\text{Cu}(\text{hfac})_2 \cdot \text{PyDPy}]_n$ were consistent with 0.375 emu/K/mol calculated for a dilute paramagnet of $S=1/2$ Cu(II). As the photolysis of the diazo group of the samples proceeded, the $\chi_{\text{mol}}T$ values started to grow and gradually leveled. As the temperature was decreased for samples **a** and **b** after completion of the photolysis, $\chi_{\text{mol}}T$ values increased continuously, reached a maximum value of 7.43 and 18.2 emu/K/mol at 14 and 3.0 K, respectively, and started to decrease somewhat toward 2 K. There were no minima observed. The behavior is reversible up until 230 K after which the $\chi_{\text{mol}}T$ values decreased sharply. In consecutive measurements on the same samples left at 300 K, the $\chi_{\text{mol}}T$ values traced the horizontal lines obtained before irradiation. The data (4–200 K) of complex **b** after irradiation for 22 h were analyzed by the method based on a model of the $S=1/2$ and $S=2/2$ Heisenberg ferromagnetic chain ($g=2$) for $[\text{Cu}(\text{hfac})_2 \cdot \text{PyCpy}]_n$ to give $J/k_B = +33.4$ K [7]. Field dependencies of magnetization M for the same sample **b** of $[\text{Cu}(\text{hfac})_2 \cdot \text{PyDPy}]_n$ at 5 K before and after irradiation gave curves in good agreement with a $S=1/2$ paramagnet and the Brillouin

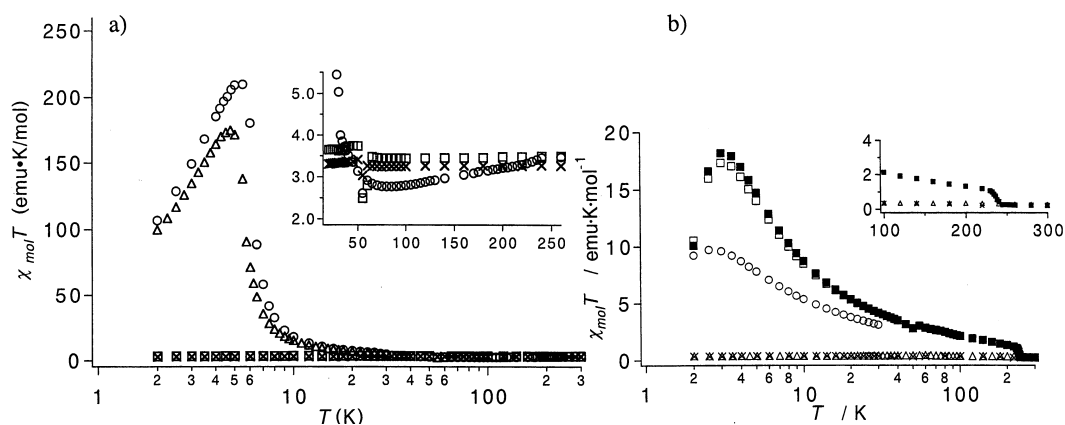


Fig. 5 Plots of $\chi_{\text{mol}}T$ vs. T for crystalline samples of (a) complex **a** of $[\text{Mn}(\text{hfac})_2 \cdot \text{PyDPy}]_n$ before (\square) and after (\circ) irradiation and (b) complex **b** of $[\text{Cu}(\text{hfac})_2 \cdot \text{PyDPy}]_n$ before (\triangle) and after (\square) irradiation.

function in which $S = 33.6 \pm 0.2$. These results correspond to the ferromagnetic coupling over ≈ 23 units at 3 K along the chains.

The observed sudden changes of the $\chi_{\text{mol}}T$ values at 240 K are understood as indicating the disappearance of the generated carbene centers by chemical reactions. The observed stability of the carbene centers is novel and most probably due to kinetic protection in the stiff crystal lattice of the metal complex.

The formation of the ferri- and ferromagnetic chains by photolysis of $[\text{Mn}(\text{hfac})_2\cdot\text{PyDPy}]_n$ and $[\text{Cu}(\text{hfac})_2\cdot\text{PyDPy}]_n$ is contrasting and best interpreted in terms of the formation of alternating units of triplet di(4-pyridyl)carbenes on the one hand and d^5 manganese(II) and d^9 copper(II) ions on the other, respectively. The observed signs of exchange coupling are consistent with those prescribed by model complexes in Tables 1 and 2.

CONCLUSION

In the $[\text{M}(\text{hfac})_2\cdot\text{NOPy}]$ -type complexes where $\text{M} = \text{Cr}(\text{III})$, $\text{Mn}(\text{II})$ and $\text{Cu}(\text{II})$, the regiospecificity in the exchange coupling is similar in sign to QDM and NOPNO when the magnetic orbital at M is π -charactered as in $\text{Cr}(\text{III})$ and $\text{Mn}(\text{II})$. The sign is reversed when magnetic orbital at M is σ -charactered as in $\text{Cu}(\text{II})$. This metal-dependent regiospecificity in the exchange coupling of the magnetic metal ion with the free radical substituent on pyridine base ligands would serve as a powerful design strategy for constructing higher dimensional extended heterospin systems.

The photochemical generation of the triplet carbene centers induces polarization of the π -electrons on the pyridine rings which in turn effects the coupling of magnetically isolated 3d spins of the $\text{Mn}(\text{II})$ and $\text{Cu}(\text{II})$ ions along the one-dimensional chains (Scheme 2). These results provide the first example of the formation of extended *ferro*- and *ferrimagnetic* chains containing photochemically generated 2p spins: a prototype of the molecular photomagnetic recording device in which only the irradiated micro domain of the non- or weakly magnetic materials becomes strongly magnetic. Once the ordering of the spins is established for samples having higher dimensional structure, the photochemically generated heterospin systems would serve as molecular photomagnetic recording devices just as photoresists become functional for printing circuit elements.

ACKNOWLEDGEMENTS

This work was supported by a Grant-in-Aid for COE Research 'Design and Control of Advanced Molecular Assembly Systems' from the Ministry of Education, Science and Culture, Japan (no. 08CE2005).

REFERENCES

- 1 H. C. Longuet-Higgins. *J. Chem. Phys.* **18**, 265–274 (1950); H. M. McConnell. *J. Chem. Phys.* **39**, 1910 (1963); M. S. Platz. *Diradicals* (W. T. Borden, ed.), Chap. 5. Wiley, New York (1982).
- 2 (a) C. J. Pedersen. *J. Am. Chem. Soc.* **79**, 2295–2299 (1957); A. R. Forrester, R. H. Thomson, G. R. Luckhurst. *J. Chem. Soc. B* 1311–1315 (1968); S. Nakazono, S. Karasawa, N. Koga, H. Iwamura. *Angew. Chem. Int. Ed. Engl.* **37**, 1550–1552 (1998). (b) A. Calder, A. R. Forrester, P. G. James, G. R. Luckhurst. *J. Am. Chem. Soc.* **91**, 3724–3727 (1969); N. Azuma, K. Ishizu, K. Mukai. *J. Chem. Phys.* **61**, 2294–2296 (1974); T. Ishida, H. Iwamura. *J. Am. Chem. Soc.* **113**, 4238–4241 (1991); F. Kanno, K. Inoue, N. Koga, H. Iwamura. *J. Phys. Chem.* **97**, 13267–13272 (1993).
- 3 K. Itoh. *Chem. Phys. Lett.* **1**, 235–238 (1967); N. Mataga. *Theor. Chim. Acta* **10**, 372–376 (1968); H. Iwamura. *Adv. Phys. Org. Chem.* **26**, 179–253 (1990); A. Rajca, S. Utamapanya. *J. Am. Chem. Soc.* **115**, 10688–10694 (1993); N. Nakamura, K. Inoue, H. Iwamura. *Angew. Chem. Int. Ed. Engl.* **32**, 872– (1993); A. Rajca. *Chem. Rev.* **94**, 871–874 (1994); K. Matsuda, N. Nakamura, K. Takahashi, K. Inoue, N. Koga, H. Iwamura. *J. Am. Chem. Soc.* **117**, 5550–5560 (1995); K. Matsuda, N. Nakamura, K. Inoue, N. Koga, H. Iwamura. *Chem. Eur. J.* **2**, 259–264 (1996).
- 4 K. Inoue, H. Iwamura. *J. Am. Chem. Soc.* **116**, 3173–3174 (1994); K. Inoue, H. Iwamura. *J. Chem. Soc., Chem. Commun.* 2273–2274 (1994); K. Inoue, H. Iwamura. *Synth. Met.* **71**, 1791–1792 (1995); K. Inoue, T. Hayamizu, H. Iwamura. *Mol. Cryst. Liq. Cryst.* **273**, 67–80 (1995); K. Inoue, T. Hayamizu, H. Iwamura. *Chem. Lett.* 745–746 (1995); T. Mitsumori, K. Inoue, N. Koga, H. Iwamura. *J. Am. Chem. Soc.* **117**, 2467–2478 (1995); K. Inoue,

- T. Hayamizu, H. Iwamura, D. Hashizume, Y. Ohashi. *J. Am. Chem. Soc.* **118**, 1803–1804 (1996); K. Inoue, H. Iwamura. *Adv. Mater.* **8**, 73–76 (1996); D. C. Oniciu, D. K. Matsuda, H. Iwamura. *J. Chem. Soc., Perkin II* 907–913 (1996); H. Iwamura, K. Inoue, K. T. Hayamizu. *Pure Appl. Chem.* **68**, 243–252 (1996).
- 5 Y. Ishimaru, K. Inoue, N. Koga, H. Iwamura. *Chem. Lett.* 1693–1694 (1994); M. Kitano, Y. Ishimaru, K. Inoue, N. Koga, H. Iwamura. *Inorg. Chem.* **33**, 6012–6019 (1994); Y. Ishimaru, H. Kumada, N. Koga, H. Iwamura. *Inorg. Chem.* **37**, 2273–2280 (1998).
- 6 M. Kitano, N. Koga, H. Iwamura. *J. Chem. Soc., Chem. Commun.* 447–448 (1994).
- 7 N. Koga, Y. Ishimaru, H. Iwamura. *Angew. Chem., Int. Ed. Engl.* **35**, 755–757 (1996); N. Koga, H. Iwamura. *Mol. Cryst. Liq. Cryst.* **305**, 415–424 (1997); Y. Sano, M. Tanaka, N. Koga, K. Matsuda, H. Iwamura, P. Rabu, M. Drillon. *J. Am. Chem. Soc.* **119**, 8246–8252 (1997); S. Karasawa, M. Tanaka, N. Koga, H. Iwamura. *J. Chem. Soc., Chem. Commun.* 1359–1360 (1997); S. Karasawa, Y. Sano, T. Akita, N. Koga, T. Itoh, H. Iwamura, P. Rabu, M. Drillon. *J. Am. Chem. Soc.*, **120**, 10080–10087 (1998).
- 8 We thank Prof. K. Morokuma of Emory University for stimulating discussions.